Article:

Escudero Castejon, L orcid.org/0000-0003-1525-0435, Sanchez Segado, S orcid.org/0000-0002-3511-0723, Parirenyatwa, S et al. (1 more author) (2016) Formation of Chromium-Containing Molten Salt Phase during Roasting of Chromite Ore with Sodium and Potassium Hydroxides. Journal for Manufacturing Science and Production, 16 (4). ISSN 0793-6648

https://doi.org/10.1515/jmsp-2016-0023

Formation of Chromium-Containing Molten Salt Phase during Roasting of Chromite Ore with Sodium and Potassium Hydroxides

L.Escudero-Castejon, S.Sanchez-Segado, S.Parirenyatwa, A.Jha

The Institute for Materials Research, School of Chemical and Process Engineering,
Faculty of Engineering, University of Leeds,
Leeds LS2 9JT (UK)

Abstract

Chromium has a wide range of applications including metals and alloys manufacturing, pigments, corrosion resistance coatings and leather tanning. The production of chromium chemicals is based on the oxidative alkali roasting of chromite ores, which leads to the formation of water-soluble alkali chromates. Previous investigations reported that when chromite is roasted with soda-ash, a molten salt containing chromium, which is mainly composed of sodium carbonate and sodium chromate (Na_2CO_3-Na_2CrO_4 binary mixture), forms under typical roasting conditions. The physical properties of the liquid phase, which are dependent on the temperature, charge and gangue compositions, play an important role on the oxidation reaction and may limit the chromate recovery by hindering the oxygen transport to the reaction interface.

This investigation focuses on the alkali roasting of chromite ore at 1000°C using NaOH and KOH, followed by water leaching. The influence of the alkali ratio on the chromium extraction yield is analysed, and the results obtained with both hydroxides are compared. Sample characterisation and thermodynamic analysis, including phase diagrams, equilibrium calculations and computation of liquidus curves, are combined with the purpose of studying the formation of the molten salt phase under different roasting conditions and its effect on the final chromium recovery.

Keywords: chromite ore, oxidative roasting, molten salt phase, NaOH, KOH, chromium recovery

1. Introduction

Le Chatelier, in the 19th century, first applied alkali roasting in oxidising conditions for the extraction of sodium chromate from chromite ores [1, 2]. This discovery formed the basis for the industrial process which is still practiced today. The application of the alkali roasting process to the extraction of different metal oxides, such as Ti, Al or V, from complex minerals has also been investigated with satisfactory results [3-9].

The process of oxidative roasting of chromite ore in the presence of alkali salts is based on the oxidation of Cr^{3+} to Cr^{6+} and subsequent combination with the alkali metal to form water soluble chromates (Na_2CrO_4, K_2CrO_4). During the traditional roasting process, chromite is reacted with sodium carbonate in oxidising conditions at a typical roasting temperature of 1100-1150^{o}C [2], to form sodium chromate following equation (1).

$$FeCr_2O_4 + 2\ Na_2CO_3 + 7/4\ O_2 \rightarrow 2\ Na_2CrO_4 + 1/2\ Fe_2O_3 + 2\ CO_2 \quad (1)$$

The roasted material is subsequently leached with water in order to selectively solubilise sodium chromate. The remaining insoluble solid, known as chromite ore processing residue (COPR), mainly contains iron oxide, magnesium oxide, insoluble silicates and unreacted chromite. The landfilling of the COPR generated is an important source of hexavalent chromium, as the waste contains approximately 0.1-0.2 wt.% Cr^{6+} which remains entrapped within the solid residue after water leaching. Hexavalent chromium is highly hazardous not only to human beings but also to aquatic environment, soil, flora and fauna [10], and therefore, the pollution-related problem associated with waste disposal is the main drawback of the alkali roasting process.

Previous investigations on alkali roasting of chromite ores have focused on the study of the thermodynamics and optimization of the process parameters in order to maximize chromium extraction and minimize toxic waste generation [11-16]. NaOH/KOH leaching of chromite ore at lower temperatures (320-400^{o}C) have also been recently developed by Zhang, Xu [17], which is based on chemical reactions similar to alkali roasting. The parameters affecting the degree of extraction include chromite ore composition, roasting temperature and time, oxygen potential and the origin and quantity of gangue materials present in the ore. Another important factor which is known to have a critical effect on the roasting reaction is the formation of an alkaline molten phase containing chromium. The formation of the alkali-rich liquid during the roasting of chromite is an important step in controlling the overall chemical reaction, which according to reaction (1) depends on the pore diffusion of oxygen. Previous findings on this topic are discussed below.

1.1. Previous findings on the role of the liquid phase in the reaction mechanism.

Tathavadkar et al. previously described the key role played by the binary Na_2CrO_4–Na_2CO_3 molten phase formed during alkali roasting of chromite ore with sodium carbonate [12]. The liquid phase mainly consists on the formation of an eutectic mixture at 928 K between Na_2CO_3 and Na_2CrO_4 with a 62.5 wt.% sodium chromate. It was pointed out that the ore composition and gangue materials have a significant effect on the properties of the binary Na_2CrO_4–Na_2CO_3 liquid phase, which ultimately affects the extraction yield of chromium. In this study, alkali hydroxides, namely NaOH and KOH, are used for the roasting of chromite ore, and therefore an M_2CrO_4-MOH molten phase, where M represents the alkali metal (Na or K), is expected to form.

When roasting with sodium or potassium hydroxide, the main reaction taking place is shown in equation (2):

$$2\ FeCr_2O_4 + 8\ MOH + 7/2\ O_2(g) \rightarrow 4\ M_2CrO_4 + Fe_2O_3 + 4\ H_2O(g) \quad (2)$$

Since chromite ore also contains iron, alumina and gangue minerals including silicates, reaction of alkali with these elements will yield new complexes which are likely to alter the chemical composition of the liquid phase. Thermodynamic analysis of the possible reactions of sodium/potassium hydroxides with the different elements of the ore (equations 3-7) shows that besides the formation of alkali chromate, formation of alkali ferrite ($NaFeO_2$, $KFeO_2$), alkali aluminate ($NaAlO_2$, $KAlO_2$) and alkali silicate (Na_2SiO_3, K_2SiO_3) is possible during roasting depending on the alkali available, as discussed somewhere else [5].

$$FeAl_2O_4 + 2\,MOH + 1/4\,O_2(g) \rightarrow 1/2\,Fe_2O_3 + 2\,MAlO_2 + H_2O(g) \quad (3)$$

$$MgAl_2O_4 + 2\,MOH \rightarrow MgO + 2\,MAlO_2 + H_2O(g) \quad (4)$$

$$Fe_3O_4 + 3\,MOH + 1/4\,O_2(g) \rightarrow 3\,MFeO_2 + 3/2\,H_2O(g) \quad (5)$$

$$MgFe2O_4 + 2\,MOH \rightarrow MgO + 2\,MFeO_2 + H_2O(g) \quad (6)$$

$$SiO_2 + 2\,MOH \rightarrow M_2SiO_3 + H_2O(g) \quad (7)$$

Previous authors [12, 18] also described the formation of the alkali compounds shown in reactions (3) to (7) which were identified either as intermediates of reaction or final products after roasting of chromite with Na_2CO_3. Tathavadkar et al. reported that the formation of $NaAlO_2$, $NaFeO_2$ and Na_2SiO_3 during roasting of chromite with Na_2CO_3 leads to a change in both the physical and chemical properties of the liquid phase [12].

The liquid phase generated acts as coating, filling the pores on the surface of the non-reacted or partially-reacted chromite particles during the oxidation reaction with alkali metal hydroxides, as shown in Figure 1. During roasting in the presence of alkali, there is diffusion of Na^+ through the liquid phase towards the reaction zone [15] and diffusion of gaseous species (O_2 and H_2O according to equation (2)). The roasting reaction is considered to be controlled by diffusion and can be described by the Ginstling and Brounshtein (GB) equation [13, 19]. In a kinetic study of alkali roasting of Indian chromite [19], it was concluded that the diffusion of Cr^{3+} and Na^+ is the rate-limiting step when temperature is low (700^{o}C to 900^{o}C), whereas at higher temperatures (above 900^{o}C) the diffusion of gaseous species controls the rate of reaction. The presence of the molten salt layer impedes the overall kinetics of sodium chromate formation when roasting at 1000^{o}C by decreasing the rate of gas diffusion (rate-limiting step) through the molten salt towards the reaction interface, where trivalent chromium is oxidised and formation of sodium chromate takes place in the presence of O_2 by reaction between Cr^{6+} and Na^+ [13, 14]. At a fixed temperature, the obstruction of the oxygen transport is more significant with increasing volume and proportion of the liquid phase in the reaction mixture.

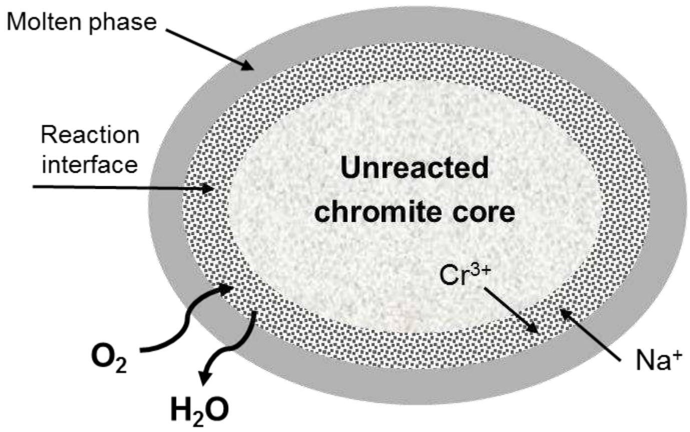

Figure 1. Schematic representation of a partially-reacted chromite particle and molten salt phase formed during roasting with alkali in oxidising conditions.

Tathavadkar et al. [12] pointed out the importance of the viscosity of the molten phase, as this is the property which mainly affects the thickness of the liquid layer and its resistance to the transport of gaseous species. In the case of roasting with Na_2CO_3, the viscosity of the Na_2CO_3–Na_2CrO_4 molten salt mixture was found to be highly dependent on the roasting temperature and the composition of the initial charge [14].

It has been demonstrated that the presence of silica leads to the formation of sodium silicate compounds which drops the activity of alkali metal ions (Na^+, K^+) and increases the viscosity of the liquid phase [12]. The differences between the reaction mechanism with and without silica are significant, and hence the yield of sodium chromate extraction strongly depends on the amount of silica present in the ore. When sodium silicate dissolves into the liquid phase, sodium ferrite and aluminate tend to dissolve too, and the result is the formation of a highly-viscous liquid rich in alkali, in which chromite dissolves completely forming a complex Na-Cr-Fe-Al-Si-Mg-O liquid at high temperature [14]. This is the reason why the presence of silica in the ore has a strong negative influence on the extraction efficiency of chromate, which is higher for ores with low silica content.

In this study, the reaction mechanism of the roasting of chromite with different ratios of NaOH/KOH has been studied. Relevant phase diagrams and equilibrium calculations were also computed with the aim of determining the different phases formed during roasting and their effect on the properties of the liquid phase, the rate of diffusion of oxygen to the reaction interface and, ultimately, the extraction efficiency of chromium.

2. Experimental part

2.1. Materials.

The South African chromite ore used in this study has a particle size of 106 μm and its chemical composition is shown in Table I. Sodium hydroxide (NaOH) and potassium hydroxide (KOH) of analytical grade were used for roasting of chromite ore samples.

Chromite ore samples were characterized using X-ray powder diffraction (XRPD), X-ray fluorescence (XRF) and scanning electron microscopy techniques (SEM). The X-ray powder diffraction pattern of the as-received chromite ore is shown in Figure 2. The main phase identified was $(Fe_{0.52}Mg_{0.48})(Cr_{0.76}Al_{0.24})_2O_4$, which corresponds to a chromite spinel phase with that particular stoichiometry. This is evident from Figure 2, where the XRPD pattern of the chromite sample and the ICDD pattern reference (01-070-6386) for the pure $(Fe_{0.52}Mg_{0.48})(Cr_{0.76}Al_{0.24})_2O_4$ phase are compared.

Table I. Chemical composition of the as-received chromite ore analysed by XRF.

Wt.%	Cr_2O_3	Fe_2O_3	MgO	Al_2O_3	SiO_2	TiO_2	CaO
Chromite ore	48.8	31.3	7.03	7.15	3.45	0.70	0.54

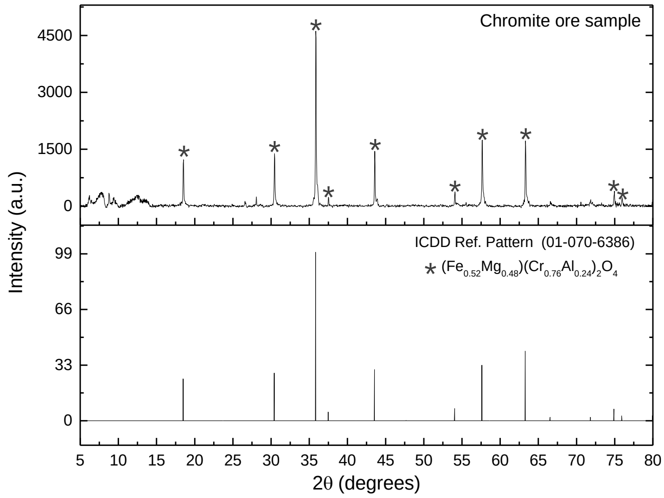

Figure 2. X-ray powder diffraction pattern of the as-received chromite ore (top) and ICDD reference pattern (01-070-6386) for the $(Fe_{0.52}Mg_{0.48})(Cr_{0.76}Al_{0.24})_2O_4$ spinel phase (bottom). Cu-Kα radiation was used (λ = 1.5418 Å).

An important factor to consider is the presence of gangue minerals in the ore, such as enstatite ($MgSiO_3$), olivine ($(Mg,Fe)_2SiO_4$), talc ($Mg_3Si_4O_{10}(OH)_2$) or serpentine ($(Mg,Fe)_3Si_2O_5(OH)_4$), among others, commonly associated with chromite ore. In this particular case, magnesium silicate with some dissolved iron and a complex Ca-Al-Na-silicate phase were identified, as shown in the backscattered SEM image and elemental mapping of the as-received chromite ore sample presented in Figure 3.

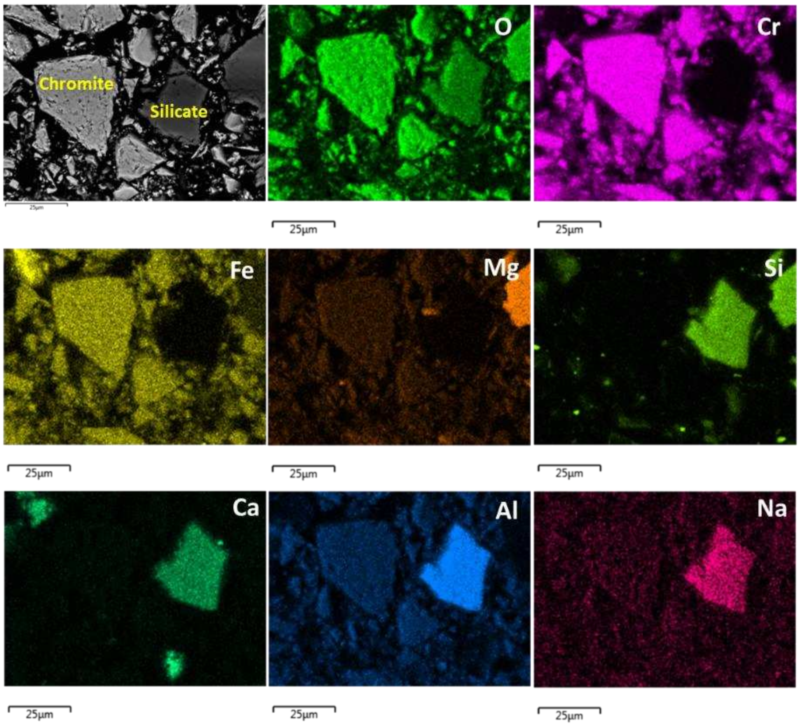

Figure 3. Backscattered scanning electron microscopy image (operating voltage = 20 kV) of the as-received chromite ore and elemental distribution map obtained from energy dispersive X-ray analysis (EDX).

2.2. Experimental procedure.

Chromite ore samples were mixed with the correspondent amount of either NaOH or KOH. The mixture was then placed inside an alumina crucible and roasted for 2 hours in a tube furnace in air atmosphere. All experiments were carried out in isothermal conditions at a temperature of 1000°C. Samples were prepared by mixing thoroughly chromite ore with different ratios of the corresponding hydroxide. The Cr_2O_3:hydroxide molar ratios tested in this study were 1:3.2, 1:4, 1:6, 1:8 and 1:10, which correspond to 80%, 100%, 150%, 200% and 250% of the stoichiometric hydroxide amount needed to convert all Cr^{3+} contained in the ore to water soluble alkali chromate (Na_2CrO_4 or K_2CrO_4).

The roasted products were water-leached for 2 hours at 50°C with the purpose of selectively separating chromium by extracting the alkali chromate into solution. Figure 4 shows the E_H-pH diagram for the Fe-Na-Cr system in water at 50°C. The striped area illustrates the conditions during the water leaching stage, where Na^+ and CrO_4^{2-} ions are found in solution leaving behind a solid residue containing insoluble phases (mainly Fe_2O_3, MgO and insoluble silicates).

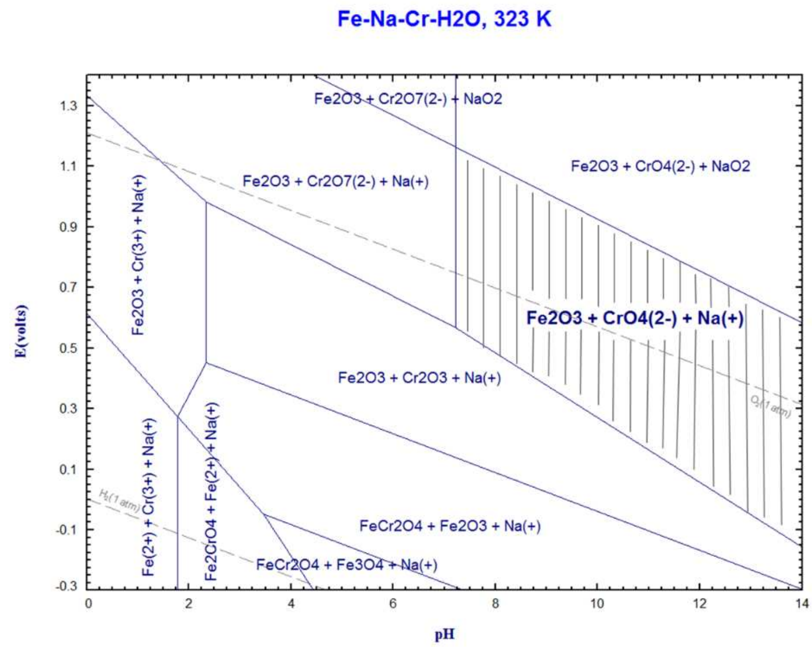

Figure 4. E_H-pH diagram for the Fe-Na-Cr-H_2O system at 323K computed using FactSage 6.4 software [20].

FactSage 6.4 software [20], including FactPS, FToxid, FTsalt and FTmisc databases, was used for computing E_H-pH and phase diagrams presented in this manuscript.

Leached solutions were analysed by atomic absorption spectroscopy (AAS) while the solid residues obtained from the leaching step were characterised by XRPD, SEM and energy-dispersive X-ray spectroscopy (EDX). For X-ray powder diffraction analysis, Cu-Kα radiation (λ = 1.5418 Å) was used and samples were examined over a 2θ angle with a maximum range of 5^o to 85^o. XRPD patterns were analysed using X'Pert HighScore Plus database software in order to identify the main phases present in the different samples.

3. Results and discussion

3.1. Thermodynamic considerations.

The effect of the alkali ratio on the oxidation reaction was studied by performing roasting experiments using five different Cr_2O_3:MOH molar ratios (where M = Na or K) of 1:3.2, 1:4, 1:6, 1:8 and 1:10. It was mentioned before that the analysis of the Gibbs free energy of the roasting of chromite with NaOH/KOH indicated that both hydroxides can be consumed by alumina and silica to form alkali aluminates and alkali silicates [5]. This makes it necessary to increase the amount of alkali above the stoichiometric, by taking into account the alumina and silica content of the ore. Iron oxide may also react with Na^+/K^+ to form $NaFeO_2$/$KFeO_2$, only if alkali is in excess.

Formation of alkali ferrites can be seen in Figure 5. The computed phase diagrams for the NaOH-Cr_2O_3-Fe_2O_3-Al_2O_3-O_2 and KOH-Cr_2O_3-Fe_2O_3-Al_2O_3-O_2 systems were calculated by using FactSage 6.4 software [20]. The diagrams indicate the phases coexisting in equilibrium at 1000°C as a function of the partial pressure of oxygen, $Pp(O_2)$, and the activity of MOH. Both diagrams show that the partial pressure of oxygen required to form the alkali chromates (M_2CrO_4) decreases as the concentration of MOH increases; implying that, from a thermodynamic point of view, chromate formation will be enhanced by the presence of excess hydroxide. It should be noticed that $NaFeO_2$ appears in Figure 5a for certain conditions of $Pp(O_2)$ and NaOH activity, whereas $KFeO_2$ does not exist in Figure 5b under comparable conditions. This is due to a lack of thermodynamic data for this compound in the software's database. However, $KFeO_2$ is expected to form if there is an excess of KOH, since the reaction for the formation of $KFeO_2$ by combination of Fe_2O_3 and KOH at 1000°C has a significantly large negative value of Gibbs energy, which is equal to ΔG_f = -1129.88 kJ per mol of reacted Fe_2O_3 at 1000°C (calculated using HSC 5.1 software [21]).

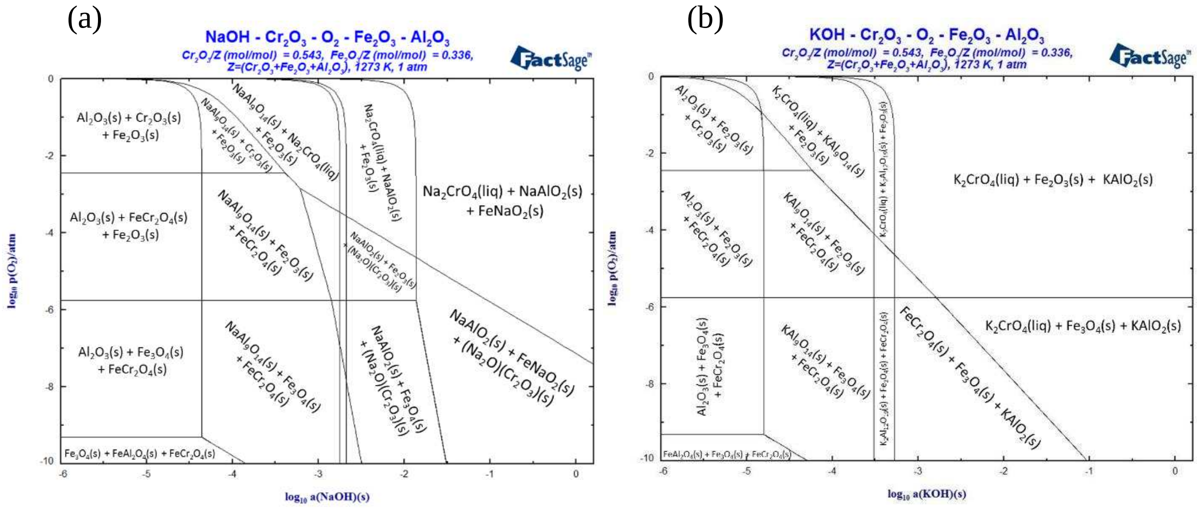

Figure 5. Phase diagrams of the a) Cr_2O_3-Fe_2O_3-Al_2O_3-NaOH-O_2 and b) Cr_2O_3-Fe_2O_3-Al_2O_3-KOH-O_2 systems. Computed using FactSage 6.4. [20].

Under conditions of high activity of the alkali compound and low partial pressure of oxygen, oxidation of Cr^{3+} to Cr^{6+} is not achieved leading to formation of alkali phases containing trivalent chromium, such as $NaCrO_2$ and $KCrO_2$; as it can be seen in Figure 5a where $(Na_2O)(Cr_2O_3)$ is found at the bottom right-hand corner of the diagram. However, $(K_2O)(Cr_2O_3)$ is not present in Figure 5b for comparable conditions of a(KOH) and $Pp(O_2)$, which may be explained due to the lack of $KCrO_2$ data in the FactSage 6.4 database. In this study, experiments were carried out in air and therefore the partial pressure of oxygen is $Pp(O_2)$ = 0.21 atm and $\log(Pp(O_2))$ = -0.68. Hence, the reaction takes place at the top of the phase diagram where the pressure of oxygen is theoretically sufficient for oxidation of chromium to (6+)-state, and $NaCrO_2$ and $KCrO_2$ are not expected to be found at equilibrium.

Phase equilibria conditions were also computed for the roasting of chromite and the five different alkali ratios tested experimentally by using FactSage 6.4 [20]. In Table II, the moles of the different phases in equilibrium after roasting 50g of chromite with the corresponding alkali amount at 1000°C are compared. As the experiments were carried out in air atmosphere, it was assumed that there was excess oxygen available.

Table II. Equilibrium data calculated for the roasting of 50g of chromite with five different ratios of NaOH/KOH (1:3.2, 1:4, 1:6, 1:8, 1:10) at 1000°C in oxidising conditions.

Alkali	Cr_2O_3:MOH	Phases in equilibrium (moles)					
NaOH	1:3.2	Na_2CrO_4 (liq) 0.24410	Fe_2O_3 0.09781	$MgAl_2O_4$ 0.02668	Mg_2SiO_4 0.01236	$NaAlSiO_4$ 0.01680	$(MgO)(Cr_2O_3)$ 0.03584
NaOH	1:4	Na_2CrO_4 (liq) 0.31425	Fe_2O_3 0.09780	$MgAl_2O_4$ 0.03368	Mg_2SiO_4 0.02643	$NaAlSiO_4$ 0.00274	$(MgO)(Cr_2O_3)$ 0.00068
NaOH	1:6	Na_2CrO_4 (liq) 0.31579	Fe_2O_3 0.01938	MgO 0.08722	$FeNaO_2$ 0.15686	$Na_6Si_2O_7$ 0.01458	$NaAlO_2$ 0.07010
NaOH	1:8	Na_2CrO_4 (liq) 0.31579	NaOH (liq) 0.24330	MgO 0.08722	$FeNaO_2$ 0.19563	Na_4SiO_4 0.02917	$NaAlO_2$ 0.07010
NaOH	1:10	Na_2CrO_4 (liq) 0.315790	NaOH (liq) 0.558800	MgO 0.087221	$FeNaO_2$ 0.19563	Na_4SiO_4 0.029167	$NaAlO_2$ 0.070098
KOH	1:3.2	K_2CrO_4 (liq) 0.24805	Fe_2O_3 0.09781	$MgAl_2O_4$ 0.03060	$MgSiO_4$ 0.01138	$KAlSi_2O_6$ 0.00890	$(MgO)(Cr_2O_3)$ 0.03387
KOH	1:4	K_2CrO_4 (liq) 0.31489	Fe_2O_3 0.09781	$MgAl_2O_4$ 0.03432	$MgSiO_4$ 0.02623	$KAlSi_2O_6$ 0.00147	$(MgO)(Cr_2O_3)$ 0.00036
KOH	1:6	K_2CrO_4 (liq) 0.31579	KOH (liq) 0.13960	MgO 0.08722	Fe_2O_3 0.09781	K_2SiO_3 (liq) 0.02917	$KAlO_2$ 0.07010
KOH	1:8	K_2CrO_4 (liq) 0.31579	KOH (liq) 0.45520	MgO 0.08722	Fe_2O_3 0.09781	K_2SiO_3(liq) 0.02917	$KAlO_2$ 0.07010
KOH	1:10	K_2CrO_4 (liq) 0.31579	KOH (liq) 0.77070	MgO 0.08722	Fe_2O_3 0.09781	K_2SiO_3(liq) 0.02917	$KAlO_2$ 0.07010

The comparison of equilibrium data in Table II and Figure 5a and b confirms that it is necessary to have excess alkali in order to extract all Cr^{3+} in the form of water soluble chromate. When the stoichiometric amount of alkali is added, part of the chromium remains unreacted as $MgCr_2O_4$, since some sodium and potassium are consumed in the formation of alkali aluminosilicates ($NaAlSiO_4$, $KAlSiO_4$). However, when excess alkali is added, the magnesiochromite phase cannot be observed in the reaction product. Based on equilibrium calculations, the majority of chromium is extracted as Na_2CrO_4 when the Cr_2O_3:NaOH molar ratio is 1:6 (150% of the stoichiometric amount), and therefore, a further increase of the amount of alkali in the charge does not necessarily mean an improvement of the chromium extraction yield. These observations were also found to be consistent with results for KOH.

Part of the alumina reacts to form $MAlSiO_4$ and the rest remains unreacted as $MgAl_2O_4$ when roasting with the stoichiometric alkali ratio, but when the ratio is increased from 1:4 to Cr_2O_3:MOH = 1:6 or above, the alumina combines with Na^+/K^+ to form sodium or potassium aluminate ($MAlO_2$). The oxides of iron and magnesium separate out by forming the respective single oxide phases (MgO, Fe_2O_3) or they may be also found combined as magnesioferrite ($MgFeO_2$). When excess alkali is high (molar ratio Cr_2O_3:MOH = 1:6 or higher), iron forms $MFeO_2$, as mentioned above.

Table II shows the state of the difference phases (solid or liquid), which allows to predict the composition of the molten salt phase. The liquid phase is mainly composed of M_2CrO_4 and unreacted MOH, however, as it can be seen in Table II, alkali silicates form when alkali is in excess (Cr_2O_3:MOH molar ratios of 1:6, 1:8 and 1:10). Particularly, if K_2SiO_3 forms during roasting, it will be present in the liquid as it melts below 1000°C (melting point of K_2SiO_3 = 976°C), leading to an increase in the viscosity of the molten phase [14]. The amount of alkali added will determine the volume of the liquid phase generated and its compositional properties for governing the intergranular fluid flow in the chromite matrix.

Eutectic diagrams for the binary systems composed by MOH or M_2CrO_4 and different alkali compounds ($MAlO_2$, M_2SiO_3, $M_2Si_2O_5$) were plotted with the aim of comparing the temperature and composition of the eutectic points of the two-component mixtures. The liquidus curves for binary phase diagrams were calculated by using the Clausius-Clapeyron relation [22], shown in equation (8), in which the liquidus temperature (T) of the binary mixture is dependent on the molar composition (x_i), by assuming that the mixture forms an ideal solution.

$$-\ln x_i = \frac{\Delta H_{fi}}{R} \cdot \left(\frac{1}{T} - \frac{1}{T_{fi}}\right) \quad (8)$$

Equation (8) allows the calculation of the theoretical liquid curves for the binary systems as a function of the heat of fusion (ΔH_f) and the melting point (T_f) of each component. The thermodynamic data required was obtained from Perry [23] and HSC 5.1 software [21]. R is the gas constant equal to 8.31 $Jmol^{-1}K^{-1}$. The computed diagrams are presented in Figure 6, where the eutectic point of each binary system is located at the intersection of the liquidus curves of the two components.

It can be seen in Figure 6a and Figure 6c that the binary mixtures M_2CrO_4 – MOH (where M is either Na or K) have the lowest temperature eutectic points with low molar fraction of the alkali chromate; 560 K – 8.2% Na_2CrO_4 and 645 K – 6.8% K_2CrO_4, respectively. The eutectic KOH – K_2CrO_4 mixture at 633 K and 7.8% K_2CrO_4 was previously reported in the literature [24, 25], which is comparable with the values obtained theoretically. The calculated eutectic temperature of the Na_2CrO_4 – NaOH mixture (560K) is significantly lower than the value for the Na_2CrO_4 – Na_2CO_3 system (928 K), which was reported in a previous study by Tathavadkar et al. [12]. It was also described on that study how the presence of other alkali compounds in the liquid phase contributes to the decrease of the eutectic temperature of the mixture, causing an increase of the liquid phase present which is detrimental for the overall oxygen transport [12].

The respective Na_2CrO_4 and K_2CrO_4 liquidus curves show that the liquidus temperature increases as the molar fraction of the alkali chromate increases, which indicates that the liquidus temperature raises as sodium hydroxide is consumed and sodium chromate is formed. NaOH and KOH form low temperature eutectics not only with the chromates but also with the rest of alkali compounds. This is shown in Figure 6b and 6d, where it can also be observed that the eutectic temperatures of the binary mixtures containing NaOH are lower than those for the binary systems containing KOH.

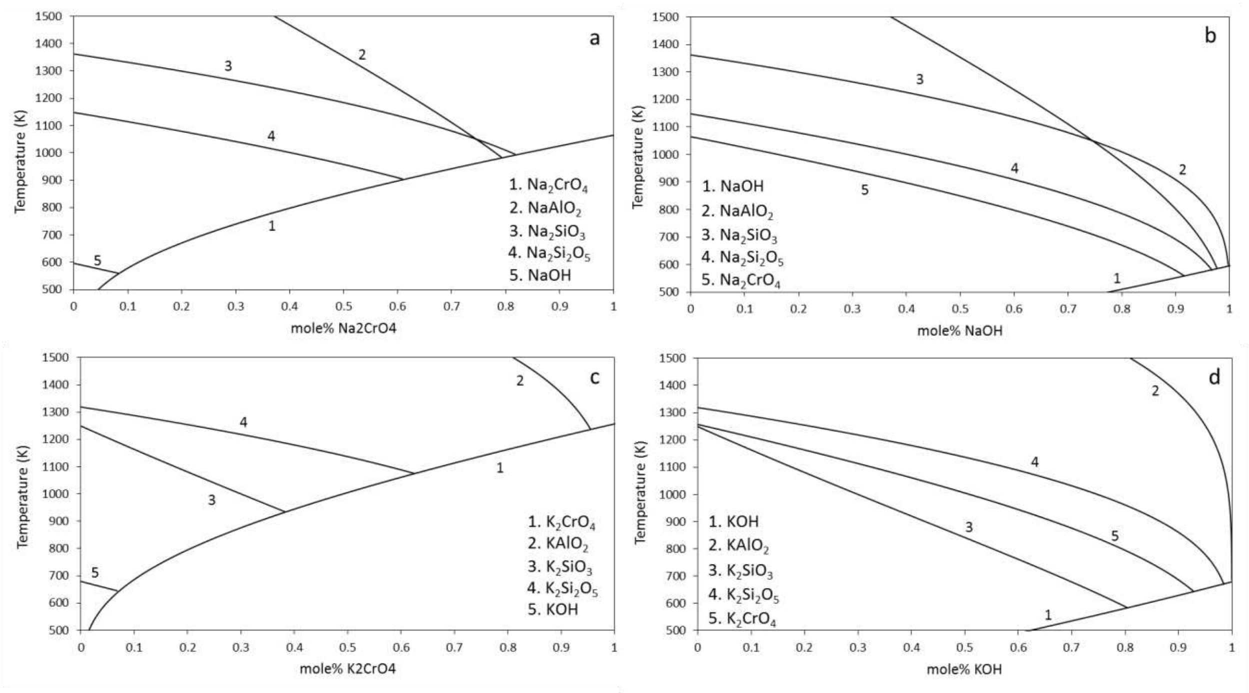

Figure 6. Liquidus curves for the A) Na_2CrO_4 and $NaAlO_2$/Na_2SiO_3/$Na_2Si_2O_5$/NaOH; B) K_2CrO_4 and $KAlO_2$/K_2SiO_3/$K_2Si_2O_5$/KOH; C) NaOH and $NaAlO_2$/Na_2SiO_3/$Na_2Si_2O_5$/Na_2CrO_4; D) KOH and $KAlO_2$/K_2SiO_3/$K_2Si_2O_5$/K_2CrO_4 binary systems.

3.2. Reaction mechanism and phase analysis.

The mechanism of the overall reaction may be analysed by combining the equilibrium data in Figure 5 and Table II with experimental results. In Figure 7, the X-ray powder diffraction data for leached residues after roasting of chromite with NaOH/KOH are compared for different stoichiometric molar ratios of Cr_2O_3:MOH (1:4, 1:6 and 1:8). Leached residues contain the insoluble phases formed during roasting, while the alkali chromate and the rest of the water soluble phases are extracted during leaching.

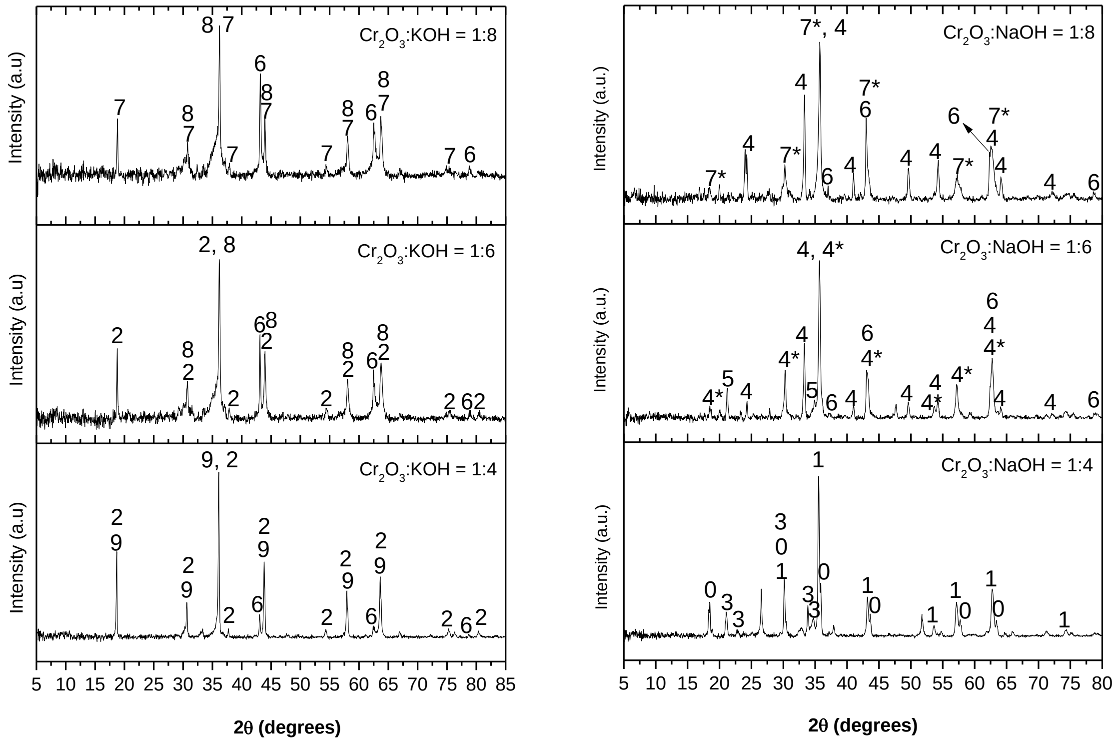

Figure 7. XRPD patterns of leached residues after roasting of chromite with different molar ratios of KOH and NaOH at 1000ºC for 2 hours. Cu-Kα radiation was used (λ = 1.5418 Å).
(0. $Mg_{0.74}Cr_{0.96}Fe_{0.26}Al_{1.04}O_4$, 1. $MgCr_{0.2}Fe_{1.8}O_4$, 2. $Mg(Fe_{0.5}Al_{0.5})_2O_4$, 3. $Na_2Mg(SiO_4)$, 4. Fe_2O_3 (hematite, rhombohedral), 4*. Fe_2O_3 (cubic), 5. SiO_2, 6. MgO, 7. $MgFe_2O_4$, 7*. $MgCr_2O_4$, 8. $Fe_{2.3}Si_{0.7}O_4$, 9. $MgCrAlO_4$)

Equilibrium data shown in Table II indicates that, for roasting of chromite with the stoichiometric Cr_2O_3:alkali molar ratio, $MgAl_2O_4$ and $MgCr_2O_4$ spinel-type phases are in equilibrium. Experimental results demonstrate that these phases are present in the core of the partially-reacted particles and are found as a complex Mg-Fe-Cr-Al-O spinel with a certain stoichiometry, which in fact corresponds to the initial chromite ore phase depleted in Fe^{2+}/Fe^{3+} species. In the XRPD patterns of the residue samples in Figure 7, the complex spinels $Mg_{0.74}Cr_{0.96}Fe_{0.26}Al_{1.04}O_4$ and $MgCr_{0.2}Fe_{1.8}O_4$ can be found when roasting with the stoichiometric amount of NaOH, and $Mg(Fe_{0.5}Al_{0.5})_2O_4$ and $MgCrAlO_4$ were present when roasting with KOH. The depletion of iron was observed in the backscattered SEM images by analysing the elemental mappings of particles from water-leached residues after roasting with the stoichiometric alkali ratio. The results are presented in Figure 8 and Figure 9 for NaOH and KOH, respectively, where it can be observed that all remaining chromium is in form of partially-reacted chromite spinel.

The edge of the particles, where chromite is in contact with oxygen, is richer in iron oxides. In agreement with the equilibrium data presented in Table II, Fe^{3+} seems to diffuse out first and remain at the edge of the partially reacted particles. This is evident in Figure 8, in which a rim of $MgFe_2O_4$ may be seen. It can also be observed in the microstructure how in some areas iron and magnesium phase-separate into the corresponding single oxide phases. Silica is mainly combined with Na^+ and Al^{3+} when roasting with NaOH (Figure 8), however, when roasting with KOH iron oxide is preferentially found as an insoluble complex K-Fe-Si-O phase, which can clearly be seen in the elemental mapping in Figure 9.

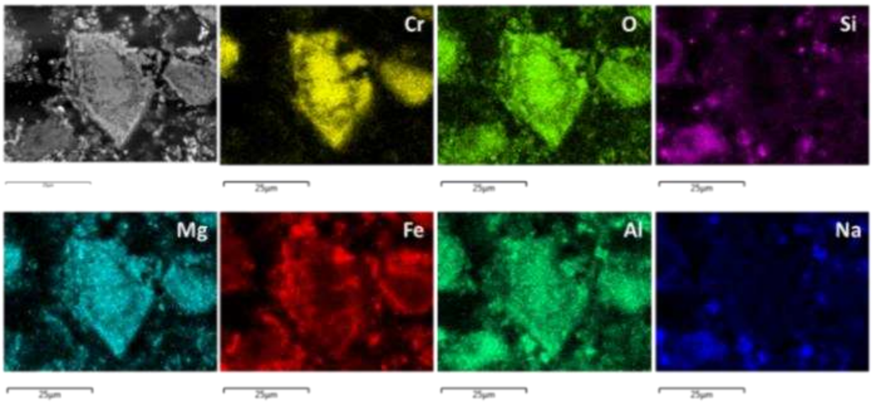

Figure 8. Backscattered SEM image and elemental distribution map obtained from energy dispersive X-ray analysis (EDX) of a leached residue particle after roasting of chromite with NaOH (Cr_2O_3:NaOH = 1:4, T = 1000°C, t = 2 hours, operating voltage = 20 kV).

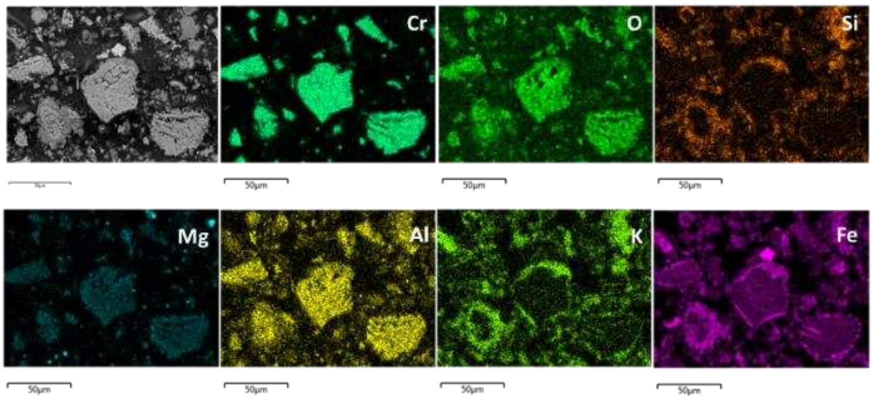

Figure 9. Backscattered SEM image and elemental distribution map obtained from energy dispersive X-ray analysis (EDX) of a leached residue particle after roasting of chromite with KOH (Cr_2O_3:KOH = 1:4, T = 1000°C, t = 2 hours, operating voltage = 20 kV).

When the molar ratio is increased to Cr_2O_3:KOH = 1:8, the water-leached residue is mainly composed of a Fe_3O_4-rich spinel phase which contains K and Si dissolved in it, which may correspond to the $Fe_{2.3}Si_{0.7}O_4$ phase identified in the XRPD patterns of Figure 7. This can be also seen in Figure 10, where a backscattered SEM image of a water-leached residue sample after roasting at 1000°C with Cr_2O_3:KOH = 1:8 is presented. Spectra at different areas were obtained by EDX and allow the comparison between the particle at the centre (spectra A and B) which corresponds to the Fe-K-Si-O phase; and the particle of unreacted chromite which can be seen at the left of the image (spectrum C).

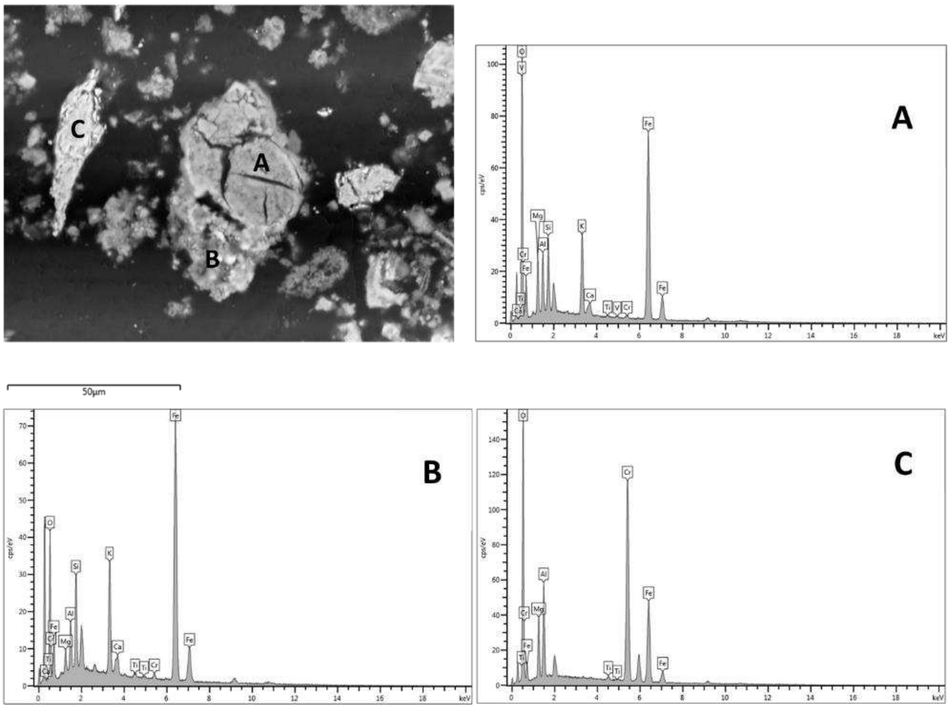

Figure 10. Backscattered SEM image and EDX spectra (A, B and C) of a leached residue particle after roasting of chromite with KOH (Cr_2O_3:KOH = 1:10, T = 1000°C and t = 2 hours, operating voltage = 20kV).

3.3. Effect of the alkali ratio on the efficiency of chromium extraction.

The concentration of chromium in the solutions obtained from the water leaching stage was analysed by AAS technique. The values of %Cr extraction for each experiment, shown in Figure 11, were calculated by using equation (9) shown below.

$$\%\,Cr\;extraction = \frac{Cr_{in\;solution}}{Cr_{in\;chromite}} \cdot 100 \qquad (9)$$

Excess alkali is expected to increase the extraction yield of chromium as a result of the following: a) equilibrium data in Table II shows the need for having higher Cr_2O_3:MOH than the stoichiometric in order to fully decompose the chromite spinel phase; b) excess alkali is necessary for neutralisation of alumina and silica and; c) phase diagrams in Figure 5 show that as the MOH concentration in the charge increases, the $Pp(O_2)$ required to form M_2CrO_4 decreases. This is in agreement with the experimental values of %Cr extraction presented in Figure 11, were the extraction of chromium increases with increasing Cr_2O_3:MOH molar ratio up to a value of 1:6. However, there is a decrease of the Cr extraction when the molar ratio is increased above 1:6, which was predicted and may be explained by the fact that a higher amount of alkali in the charge increases the volume of molten salt phase present in the reaction mixture. A higher volume of liquid represents an increase of the physical resistance to pore diffusion of gaseous species towards the reaction interface, and therefore, a decrease of the alkali chromate formation, as seen in Figure 11. The maximum chromium extraction yields obtained were 91.1% and 88.51% when roasting chromite with NaOH and KOH (Cr_2O_3:MOH = 1:6), respectively.

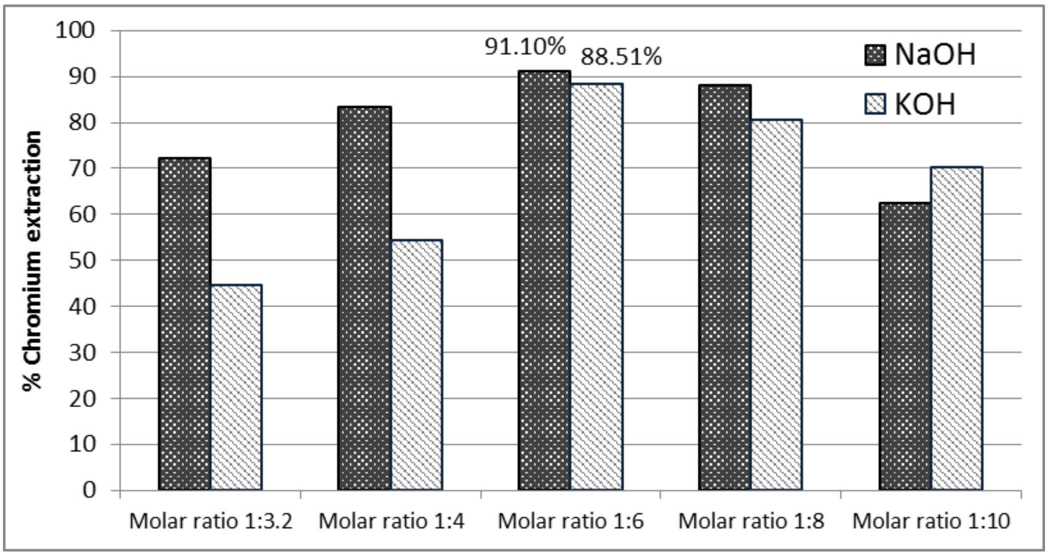

Figure 11. %Cr extraction after roasting of chromite at 1000°C with different Cr_2O_3:MOH ratios, followed by water leaching.

Conclusions

Phase diagrams for the MOH-Cr_2O_3-Fe_2O_3-Al_2O_3-O_2 systems (M=Na/K) were computed, showing the effect that the Pp(O_2) and the activity of the alkali compound have on the equilibrium phases formed. Thermodynamic equilibrium calculations were also performed for the roasting of chromite with different Cr_2O_3:MOH molar ratios (1:4, 1:6 and 1:8) for verifying the presence of the various phases formed and predict the composition of the molten phase in equilibrium. Equilibrium data showed the need for having higher Cr_2O_3:MOH than the stoichiometric in order to fully decompose the chromite spinel phase and confirmed that formation of alkali ferrites, aluminates and silicates is possible and may influence the properties of the molten salt.

The reaction mechanism with different alkali ratios was discussed based on experimental results and thermodynamic data, which were in good agreement. The main phases found in water leached residues were: partially-reacted chromite, Fe_2O_3, MgO and complex silicates. Sodium chromate was not present in water leached residues as shown by XRPD and SEM results, which suggests high efficiency of the leaching step. It was shown that the addition of excess alkali increases the extraction of chromium but it also generates a higher volume of molten phase, leading to lower reaction rates as it represents an obstacle to the pore diffusion of oxygen.

Acknowledgements

The authors acknowledge the financial support from the EPSRC standard grants (GR/T08074/01 and GR/L95977/01) and PhD studentships for research which were initiated in 1997 at the University of Leeds. AJ also acknowledges the support from the European Union's Marie Curie Fellowship grant number 331385 for Dr. Sanchez-Segado and from the NERC's Catalyst Grant reference NE/L002280/1.

References

1. Jha, A., The alkali roasting of complex oxide minerals for high purity chemicals-beyond the Le Chatelier era into the 21st century. JOM, 2011. **63**(1): p. 39-42.
2. Maliotis, G. and W.P. Industrial Minerals Information Ltd., Chromium uses & markets Statistical supplement. 1996.
3. Foley, E. and K.P. MacKinnon, Alkaline roasting of ilmenite. Journal of Solid State Chemistry, 1970. **1**(3): p. 566-575.
4. Nafeaa, I., et al., Kinetic Study of Formation of Sodium Titanets by Roasting of Soda Ash and Ilmenite Ore Concentrate. Indian Chemical Engineer, 2013. **55**(4): p. 283-293.
5. Parirenyatwa, S., et al., Comparative study of alkali roasting and leaching of chromite ores and titaniferous minerals. Hydrometallurgy, 2015.
6. Sanchez-Segado, S., A. Lahiri, and A. Jha, Alkali roasting of bomar ilmenite: rare earths recovery and physico-chemical changes. Open Chemistry, 2015. **13**(1).
7. Sanchez-Segado, S., et al., Reclamation of reactive metal oxides from complex minerals using alkali roasting and leaching–an improved approach to process engineering. Green Chemistry, 2015. **17**(4): p. 2059-2080.
8. Tathavadkar, V., M. Antony, and A. Jha. Improved extraction of aluminium oxide from bauxite and redmud. in LIGHT METALS-WARRENDALE-PROCEEDINGS-. 2002. TMS.
9. Tathavadkar, V. and A. Jha. The effect of molten sodium titanate and carbonate salt mixture on the alkali roasting of ilmenite and rutile minerals. in VIIInternational Conference on Molten Slags Fluxes and Salts, The South African Institute of Mining and Metallurgy,[2004],(255-261). 2004.
10. Nickens, K.P., S.R. Patierno, and S. Ceryak, Chromium genotoxicity: a double-edged sword. Chemico-biological interactions, 2010. **188**(2): p. 276-288.
11. Antony, M.P., et al., Recovery of chromium from industrial wastes, in Environmental Issues and Waste Management in Energy and Mineral Production Singhal Raj K. and Mehrotra Anil K., Editors. 2000, Balkema, Rotterdam. p. 751-755.
12. Tathavadkar, V., A. Jha, and M. Antony, The effect of salt-phase composition on the rate of soda-ash roasting of chromite ores. Metallurgical and Materials transactions B, 2003. **34**(5): p. 555-563.
13. Tathavadkar, V., A. Jha, and M. Antony, The soda-ash roasting of chromite minerals: Kinetics considerations. Metallurgical and Materials Transactions B, 2001. **32**(4): p. 593-602.
14. Tathavadkar, V.D., The process physical chemistry of extraction of sodium chromate from chromite ores. 2001, Ph.D Thesis, University of Leeds.
15. Sanchez-Segado, S. and A. Jha, Physical Chemistry of Roasting and Leaching Reactions for Chromium Chemical Manufacturing and Its Impact on Environment-A Review, in Materials Processing Fundamentals. 2013, John Wiley & Sons, Inc. p. 225-236.
16. Li, P., et al., Phase transformation and structure evolution of chromite in the late stages of soda ash roasting process. Mineral Processing and Extractive Metallurgy, 2016. **125**(2): p. 64-70.
17. Zhang, Y., et al. A Clean Production Process of Chromic Oxide. in The 2008 Annual Meeting. 2008.
18. Qi, T.-g., et al., Thermodynamics of chromite ore oxidative roasting process. Journal of Central South University of Technology, 2011. **18**: p. 83-88.

19. Antony, M., V. Tathavadkar, and A. Jha, Alkali roasting of Indian chromite ores: thermodynamic and kinetic considerations. Mineral processing and extractive Metallurgy, 2006. **115**(2): p. 71-79.
20. Bale, C., A. Pelton, and W. Thompson, FactSage 6.4, Factsage thermochemical software and databases.
21. Roine, A. and H. Outokumpu, Chemistry for Windows: Chemical Reaction and Equilibrium *Software with Extensive Thermodynamical Database, Version 5.1, User's Guide.* Outokumpu Research Oy, Finland, 2002.
22. Haasen, P., Phase transformations in materials. 1991: Wiley-VCH.
23. Perry, D.L., Handbook of inorganic compounds. 2016: CRC press.
24. Reshetnikov, N. and N. Vilutis, Fusibility Diagrams of some Binary Systems of Alkali Metal Hydroxides and Salts. Zhur. Neorg. Khim, 1958. **3**: p. 177.
25. Janz, G.J., et al., Physical properties data compilations relevant to energy storage. I. Molten salts: eutectic data. 1978, Manchester Coll. of Science and Technology (UK). Dept. of Chemistry.